

# Needles from Haystacks: The Search for the Lepton Flavor-Violating Decay $\tau \rightarrow \mu\gamma$

David Strozzi

*Department of Physics,*

*Princeton University*

Advisor: Dr. Daniel Marlow

Second Reader: Dr. Eric Prebys

## Abstract

In this paper, I study the prospects for detecting the lepton flavor-violating decay  $\tau \rightarrow \mu\gamma$ . Although lepton flavor conservation is a central principle of the Standard Model, some extensions to the theory, such as supersymmetry and string theory, predict that this conservation law is not exact. An extensive search for this decay at the CLEO detector found no candidate events in  $1.4 \times 10^6$   $\tau$  pairs, and placed an upper limit of  $4.2 \times 10^{-6}$  on its branching ratio at 90% confidence level. An experiment planned to take place at the BELLE detector in KEK, Japan will examine a much larger number of  $\tau$  pairs,  $\sim 10^8$ . I present here a data analysis process that admitted 9 background  $\tau \rightarrow \mu\gamma$  events in a Monte Carlo simulation of the experiment, with a signal acceptance of 19.3%. Given these results, the BELLE experiment should detect a  $\tau \rightarrow \mu\gamma$  branching ratio of  $2.7 \times 10^{-7}$  at 90% confidence level, well below the CLEO upper limit.

# 1 Overview

Over the past three centuries, a coherent framework containing almost all our knowledge of fundamental physics has evolved. Dubbed the “Standard Model” (SM), this theory provides a so-far empirically correct account of all the particles observed in nature and their interactions, with the only exception being gravity. As successful as this theory is, there are strong reasons to believe it is incomplete. First, gravity has yet to be included in the theory the way the strong, weak, and electromagnetic interactions have been. Within the SM itself, the origin of mass is still a largely open question, with most physicists favoring the Higgs Mechanism as the solution. Cosmology also offers suggestions that the SM must be extended. In particular, cosmologists do not understand how to account for the density fluctuations in the early universe needed to produce its current structure of matter clumped into galaxies, with one popular solution being “dark matter,” or particles not yet included in the SM.

Some of the currently fashionable extensions to the SM question some of its conservation laws. For instance, the SM holds that a quantity called lepton flavor is conserved in all interactions, but supersymmetry and some forms of string theory hold that this quantity is not exactly conserved [1],[2]. Recently, efforts have been made to detect the lepton-flavor violating process  $\tau \rightarrow \mu\gamma$ . An experiment on the CLEO II detector at the Cornell Electron Storage Ring (CESR) produced  $1.4 \times 10^6$   $\tau$  pairs and placed an upper limit of  $4.2 \times 10^{-6}$  on the branching ratio for this decay at 90% confidence level [3]. An experiment at the Japanese BELLE detector, scheduled for the near future, will examine  $10^8$   $\tau$  pairs for this decay. In this paper, I present an analysis of the upper limit estimate which the BELLE experiment can establish. I develop a procedure for detecting  $\tau \rightarrow \mu\gamma$  decays, including cuts to eliminate background events. I then simulate this experiment computationally to optimize the signal-to-noise ratio of these cuts and determine how many background events they will admit. The resulting set of cuts registered 9 background events from the simulation and accepted 19.3% of signal events, i.e., events where  $\tau \rightarrow \mu\gamma$  occurred.

## 2 The Standard Model and Lepton Flavor

Broadly speaking, the SM provides a scheme for classifying the known particles and their interactions. The fundamental particles are divided between fermions and bosons, with the fermions subdivided into the quark and lepton sectors. The lepton sector consists of three flavors or generations, each containing a massive lepton with electric charge -1 and a companion neutrino. The massive leptons, in order of increasing mass, are the electron (denoted by  $e^-$ ), the muon ( $\mu$ ), and the tau lepton ( $\tau$ ). The three flavors of neutrinos ( $\nu_e, \nu_\mu$ , and  $\nu_\tau$ ) are all thought to be massless, although the SM neither requires this nor offers any fundamental insight into why this should be. We will see below that the neutrino masses relate to a phenomenon called generation mixing, which occurs in the quark but has not yet been observed in the lepton sector. Other than the fact that all quarks are massive, the quark sector is structured in exactly the same way as the lepton sector, with the three generation being (up, down), (charm, strange), and (top, bottom). We can represent this scheme as follows:

$$\text{quarks : } \begin{pmatrix} u \\ d \end{pmatrix} \begin{pmatrix} c \\ s \end{pmatrix} \begin{pmatrix} t \\ b \end{pmatrix}, \quad \text{leptons : } \begin{pmatrix} \nu_e \\ e \end{pmatrix} \begin{pmatrix} \nu_\mu \\ \mu \end{pmatrix} \begin{pmatrix} \nu_\tau \\ \tau \end{pmatrix}.$$

Besides simply classifying particles, the SM also describes how they interact. The fermions mentioned above interact by the exchange of the various fundamental bosons, called gauge bosons. Each of the basic interactions is said to be mediated by certain gauge bosons: photons ( $\gamma$ ), gluons, and the massive  $W^\pm$  and  $Z^0$  particles mediate the electromagnetic, strong, and weak force, respectively. The SM includes a beautiful procedure for determining the form of the interaction between fermions and gauge bosons. One starts by constructing the Lagrangians for the free propagation of the relevant fermions and bosons, which describe how each kind of particle behaves “by itself.” One then demands that the Lagrangian is invariant under some transformation, called a symmetry. This condition can only be satisfied if a term is added to the Lagrangian involving the wavefunctions of both the fermions

and bosons — the so-called interaction term. One exploits this mechanism to find the Lagrangians for the electromagnetic, weak, and strong interactions, indicating a deep similarity between these three forces.

Nowhere is this process more straightforward and well-understood than in electromagnetism. We start with the Lagrangian  $L_M$  for Maxwell’s equations in free space, which describes free photons, and  $L_D$  for the Dirac equation, which is the relativistic equation of elementary spin-1/2 particles. We then demand that the combined Lagrangian  $L_{Tot} = L_D + L_M + L_{Int}$  is invariant under the transformation  $\psi \rightarrow \exp[i\alpha[\vec{x}]]\psi$  (in this paper,  $\vec{x}$  denotes a four-vector and  $\mathbf{x}$  a three-vector). This symmetry, called “local gauge invariance,” merely states that changing the phase of  $\psi$ , by a different amount at every point in spacetime, should have no effect on the equations of motion. This can be satisfied by a unique choice of  $L_{Int}$  (up to the usual gauge invariance in the electromagnetic potential  $\vec{A}$ ), and the resulting  $L_{Tot}$  yields the quantum-mechanical analog of Maxwell’s equations in regions of charge, or the interaction of electrons and photons. Of course, Maxwell’s equations conserve charge, and so do the equations of motion implied by  $L_{Tot}$ . However, we can foresee this before constructing  $L_{Int}$  thanks to Emmy Noether’s famous 1917 theorem connecting symmetries and conservation laws ([4], App. F). Noether proved that a symmetry of the Lagrangian is equivalent to a conserved quantity. We now understand electric charge conservation not as fundamental in its own right, but as a consequence of the local gauge symmetry we impose on the Lagrangian.

Local gauge invariance is considered a necessary symmetry of the Lagrangian describing all the interactions in the SM. For the electromagnetic force, this symmetry manifests itself in charge conservation, which is therefore seen as a fundamental conservation law. There are, however, other conservation laws which do not stem from local gauge invariance or any other “natural” symmetry of the Lagrangian. Instead, one must modify the SM in some way which amounts to explicitly tacking on the needed symmetries. A prime example of this is flavor conservation. Although this “artificial” conservation law holds in the lepton sector,

it is noticeably violated in the quark sector. The SM includes a formalism by which the weak interaction can change quark flavor, or the net number of quarks from each generation present. The basic idea is that the quark eigenstates of the weak interaction are not identical to the mass eigenstates. The electromagnetic  $L_{int}$  contains the 4-current of electrons,  $j^\mu \equiv \bar{\psi}\gamma^\mu\psi$ , where  $\psi$  is now a 4-vector and  $\gamma^\mu$  a  $4 \times 4$  matrix. The exact meaning of the overbar and the  $\gamma$  matrices stem from the Dirac equation and are not important for us, so we will omit them. The weak  $L_{Int}$ , on the other hand, deals with a 3-vector of 4-currents, one for each flavor of quark or lepton:

$$\mathbf{J}_w = (\bar{u}, \bar{c}, \bar{t})M_q \begin{pmatrix} d \\ s \\ b \end{pmatrix}, \quad (1)$$

where each letter represents the wavefunction for a given quark. We use the six quarks here, but the same current describes lepton interactions if one replaces the column vector with  $(e, \mu, \tau)$  and the row vector with the corresponding neutrinos.  $M_q$  denotes a  $3 \times 3$  unitary matrix ( $M_q^\dagger = M_q^{-1}$ ), called the mixing or Kobayashi-Maskawa (KM) matrix, and allows for generation mixing. The wavefunctions in the column vector are not weak but mass eigenstates; the KM matrix specifies how to write the former as linear combination of the latter. For instance, the weak eigenstate of the down quark  $d_w = M_{11}d + M_{12}s + M_{13}b$ .

That  $M_q$  is nondiagonal has been well-established in numerous experiments where quark flavor is indeed not conserved, such as Kaon decay. While the SM clearly allows for a nondiagonal  $M_q$ , this fact does not stem from any general principle within the theory but must be inserted *ad hoc*. More importantly, the SM offers little insight into why the KM matrix has the values it does, or what the values should be for an analogous “lepton KM matrix”  $M_l$ . One insight the SM does offer is that exactly massless neutrinos would suppress “horizontal” transitions, such as  $\tau \rightarrow \mu\gamma$ . To see this, we first note that such transitions in the quark sector, for instance  $d \rightarrow s$ , are made possible by processes that involve weak

neutral currents, and thus the  $Z^0$  boson. A precise calculation of the cross-sections for these processes involves quantum field theory and is not of interest here [5],[4]. The relevant upshot of such an analysis is the GIM mechanism, which stipulates that the unitarity of  $M_q$  and identical  $u$ ,  $c$ , and  $t$  quark masses would completely suppress this diagram. The current SM holds that  $M_q$  is indeed unitary, but the quark masses are different. In the lepton sector, we can contemplate exactly the same process and draw the same conclusions. However, the neutrino masses are known to be either tiny or zero, implying that the mass difference between different flavors is small. This means that the neutrino masses obscure the values of  $M_l$ , and will prevent many lepton flavor-violating decays that may otherwise be possible.

### 3 Data Acquisition and Analysis

In order to study the decay of the  $\tau$ , we need to produce a large number of them in a detector. The BELLE detector produces particles by colliding an  $e^+$  and an  $e^-$  beam. Most of the time, the two particles will simply Rutherford scatter off each other. However, as with any particle-antiparticle pair, there is a cross-section for them to annihilate and produce a photon. In the  $e^+e^-$  center-of-mass frame (CM), this event consists of two particles colliding with equal and opposite 3-momenta and producing a photon. Since total 4-momentum is conserved, and since the total 3-momentum is 0 before the collision (this condition defines the CM frame), the total 3-momentum must also be 0 afterwards. But the only particle present afterwards is the photon, which must travel with speed  $c$  in the CM (or any other inertial) frame, so the total 3-momentum afterwards cannot be 0. If this process is kinematically forbidden, how can it happen at all? The perspective of quantum electrodynamics is that a particle can have any mass necessary for the process under consideration, but how much this can differ from its “nominal” mass depends on how long it exists. We can therefore contemplate a photon at rest in the CM frame which abides for only a short time and then decays. Such a photon is called a virtual photon ( $\gamma^*$ ), and is said to be off its mass shell

(since it must have nonzero mass to be at rest in the CM frame). In principle, any photon that is emitted and then absorbed by another particle can also be considered virtual, but the longer it persists the less off its mass shell it can be, and for sufficiently large times the distinction between virtual and real photons is semantic.

To conserve energy, the virtual photon must decay into a particle whose total energy equals the sum of the CM energies of the two incoming particles. The energies of the  $e^-$  and  $e^+$  in the lab frame for the BELLE detector are  $E_- = 7.996$  GeV and  $E_+ = 3.5$  GeV, respectively. At these energies we can safely approximate the particles as massless, giving a combined invariant mass of  $10.58$  GeV/ $c^2$  (see discussion below). I adopt the common practice of working in units where  $c = 1$ , so that masses are measured in energy/ $c^2$  and momenta in energy/ $c$ . The invariant mass is both a Lorentz invariant and a conserved quantity in all collisions, so the CM energy of the virtual photon's decay daughters will be  $10.58$  GeV. Since the  $\tau$  rest mass is  $1.777$  GeV/ $c^2$ , it is possible for the photon to decay into a  $\tau^+\tau^-$  pair — this process respects all known conservation laws. This will provide us with  $\tau$  particles.

Having a mechanism to produce  $\tau$ 's, we now need a way to determine when a virtual photon is produced and indeed decays into a  $\tau$  pair. First note that given CLEO's upper limit of  $4.2 \times 10^{-6}$  on the branching ratio, the probability of a  $\tau$  pair being produced, and both decaying into a  $\mu\gamma$  pair, is at most  $1.8 \times 10^{-11}$ . Therefore, we assume that in an event where one  $\tau$  decays to  $\mu\gamma$ , the other  $\tau$ , called the spectator, will decay through an already-known channel. In a real sense, then, an event where both  $\tau$ 's decay to  $\mu\gamma$  is *not* a signal event. We select 7  $\tau$  decay modes which together account for 95.9% of the branching ratio, and look for the end-products of one of these decays plus  $\tau \rightarrow \mu\gamma$  in the detector's output (see table 1). In a more thorough analysis, we could increase this number slightly by including kaon decay modes, which are identical to those of the pion ( $\pi$ ) but with much smaller branching ratios. We list the decays in the case that the  $\tau^+$  is the spectator, but we also detect the same modes of the  $\tau^-$ . We do this by requiring that the number of each particle type (matter or antimatter) equals those for one of the 7 modes, and that the total

Table 1: Detected Decay Modes.

$\tau^+$ spectator decay	Branching ratio (%)	Observed final state
$\pi^+\pi^0\bar{\nu}_\tau$	25.24	$\mu^-\pi^+3\gamma$
$e^+\bar{\nu}_\tau\nu_e$	17.83	$\mu^-e^+\gamma$
$\mu^+\bar{\nu}_\tau\nu_\mu$	17.35	$\mu^-\mu^+\gamma$
$\pi^+\bar{\nu}_\tau$	11.31	$\mu^-\pi^+\gamma$
$\pi^+(\geq 2)\pi^0\bar{\nu}_\tau$	9.8	$\mu^-\pi^+(\geq 5)\gamma$
$2\pi^+\pi^-\bar{\nu}_\tau$	9.44	$\mu^-\pi^+\pi^+\pi^-\gamma$
$2\pi^+\pi^-(\geq 1)\pi^0\bar{\nu}_\tau$	4.88	$\mu^-\pi^+\pi^+\pi^-(\geq 3)\gamma$

end-product charge is 0. The  $\tau$  lifetime of  $2.4 \times 10^{-13}$  s guarantees that almost every  $\tau$  will decay well before reaching the walls of the detector ( $\sim 2$  m from the  $e^+e^-$  collision region). The  $\pi^0$  has a minute lifetime ( $\sim 8.4 \times 10^{-17}$  s) and will almost certainly decay into 2  $\gamma$ 's before leaving the detector, while the  $\mu$  lifetime is long enough (2.2  $\mu$ s) that it will almost certainly reach the detector before decaying. These facts, along with the incredibly weak interaction of neutrinos with matter, leads to the ‘‘observed final state’’ column in table 1.

To implement our analysis, we need to differentiate between charged  $\pi$ 's,  $\mu$ 's,  $e$ 's, and  $\gamma$ 's, and to measure their momenta. Fig. 1a presents a schematic of the BELLE detector, and technical information is given in [6]. The detector measures charged particle momenta through the central drift chamber (CDC) which surrounds the region where the initial  $e^+e^-$  collision takes place. A drift chamber consists of an array of wires immersed in an easily-ionized gas, with an equal hydrogen-ethane mixture used in BELLE. Charged particles ionize the gas as they pass through it, leaving behind a streak of ionized particles along their trajectory. A weak electric field moves the liberated electrons to a negative anode wire at a well-known drift velocity. A particle produced in the initial  $e^+e^-$  collision is typically so energetic as to be moving very near  $c$ , so we can safely estimate the time it is created as the time it first interacts with detectors beyond the CDC, such as the electromagnetic calorimeter. Knowing the time of the particle's creation and the electron drift velocity, we

can determine how far a particle's track is from an anode that receives these electrons. We can then place a circle around each wire, representing the track's distance from it, and then fit a track to touch all the circles. A magnetic field also threads through the CDC, causing charged particles' paths to curve. The Lorentz force law remains valid in special relativity, giving  $pc = qBR$  in gaussian units. The charge is  $\pm 1$  for every charged particle we observe (i.e., everything except free quarks), and since we control the direction of the  $B$ -field, we can deduce the charge from the direction of curvature. If we know the charge we can determine  $p$ , the momentum transverse to the magnetic field by measuring the radius of curvature  $R$ . The particle's total momentum deviates slightly from this, and special techniques such as placing a few of the CDC wires skew relative to the rest of the array exist to measure this effect.

The CDC may tell us the momentum of charged particles, but we need to use other equipment to study photons and to determine the type of particle. The CDC is surrounded by CsI(Tl) crystals which constitute the electromagnetic calorimeter (ECAL). As photons pass through a crystal, they lose almost all of their energy by  $e^+e^-$  pair production, which in turn heats the crystal. Besides the photon's energy, we can also resolve the direction of photon motion to be within the segment of solid angle subtended by the crystal. Charged particles lose energy via ionization and occasional nuclear collisions, but tend not to lose much of their energy. The notable exception to this is the electron: because it has a high cross-section for emitting bremsstrahlung photons when near nuclei, it will lose almost all its energy in the ECAL. We can distinguish an electron from a photon by whether a track appears in the CDC that connects to the crystal which the particle in question hit. The last challenge is to difference between muons and pions. After passing through the ECAL, these particles encounter a series of iron sheets interleaved with detector layers, called the iron flux-return yoke. Energetic muons will tend to pass through the iron, while the pions will engage in strong interactions with the iron nuclei and therefore survive for only a few layers on average.

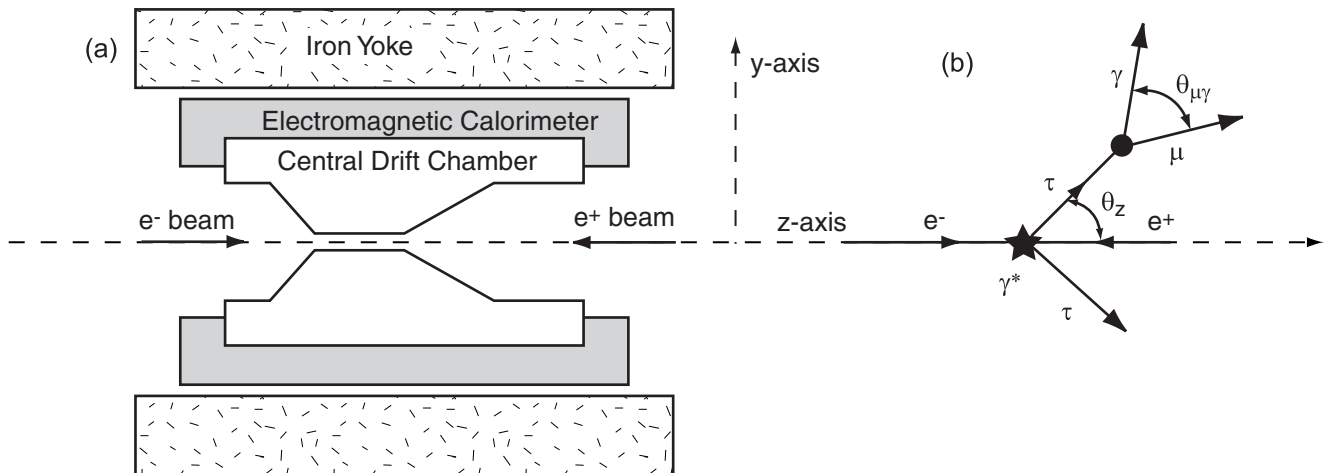


Figure 1: Diagram of BELLE Detector and kinematic geometry.

I now describe how to identify a signal event as such. I discard any events where one of the final states in table 1 is not observed in the detector. For each remaining event, I identify all possible  $\mu\gamma$  pairs and store certain measured parameters for the pair. Since many of the  $\gamma$ 's originate from a  $\pi^0$  decay, I eliminate from the list of  $\gamma$ 's any pairs that reconstruct to the  $\pi^0$  invariant mass. Any pairs which meet certain kinematic conditions are considered  $\tau \rightarrow \mu\gamma$  events. I simulate the experiment assuming the current SM, which forbids  $\tau \rightarrow \mu\gamma$ . The number of events surviving my cuts represents the background number of events that should pass through *if  $\tau \rightarrow \mu\gamma$  does not occur*. This number is crucial to the statistics of measuring the  $\tau \rightarrow \mu\gamma$  branching ratio (see below).

I base my cuts on the  $\mu\gamma$  pairs on relativistic kinematics, using the geometry depicted in fig. 1b. The first cut pertains to the invariant mass of the  $\mu\gamma$  system. Recall from special relativity that if a particle of energy  $E$  moves with 3-velocity  $\mathbf{v}$  in an inertial frame of reference, its 4-momentum is defined as

$$\vec{p} \equiv (E, \mathbf{p}), \quad \text{where } E \equiv \gamma m, \quad \mathbf{p} \equiv \gamma m \mathbf{v}, \quad \text{and } \gamma \equiv \sqrt{1 - v^2} \quad (2)$$

(remember that I work in units where  $c = 1$ ). The magnitude of a 4-vector such as momentum is defined by  $|\vec{p}|^2 \equiv E^2 - \mathbf{p}^2$ , which ensures that it is Lorentz invariant (or the same in all

inertial frames). Weak interactions, along with all other known interactions, conserve 4-momentum, that is,  $\vec{p}_b = \vec{p}_a$ , where  $\vec{p}_b =$  total 4-momenta before interaction and  $\vec{p}_a =$  total 4-momenta afterwards. In particular, this implies that their magnitudes are equal:  $|\vec{p}_a| = |\vec{p}_b|$ . For the  $\tau \rightarrow \mu\gamma$  decay,

$$\vec{p}_b = \vec{p}_\tau = \gamma m_\tau (1, \mathbf{v}) \implies |\vec{p}_b| = \gamma m_\tau \sqrt{1 - v^2} = m_\tau. \quad (3)$$

This gives us a powerful cut: in any inertial frame (such as the lab frame),  $|\vec{p}_\mu + \vec{p}_\gamma| = m_\tau$ .

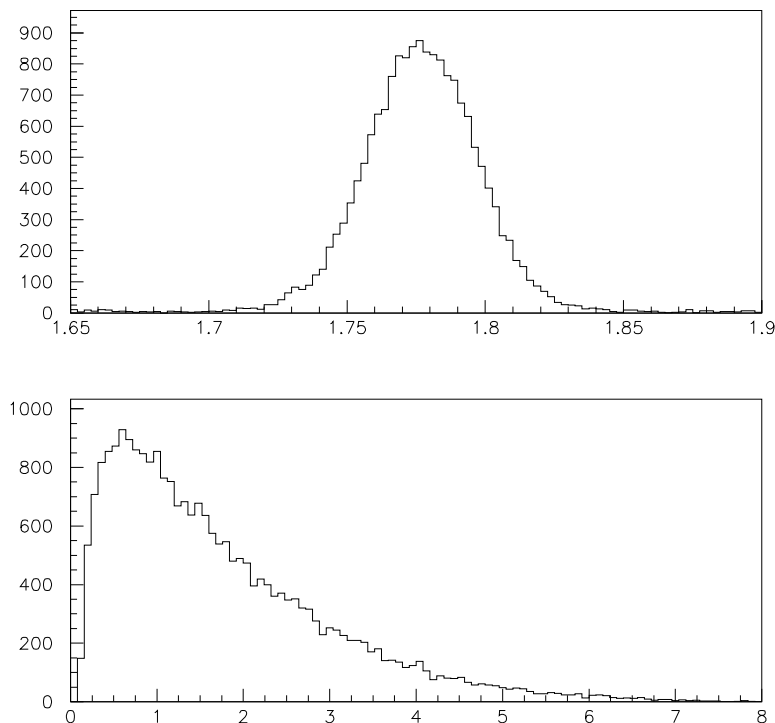


Figure 2: Invariant mass spectrum ( $\text{GeV}/c^2$ ), signal above background.

I now need to translate this condition into a constraint on empirically measured parameters. We can identify muon tracks as such, so we know their mass. We can also measure

the  $\mu$  and  $\gamma$  3-momenta vectors. Defining  $M \equiv |\vec{p}_\mu + \vec{p}_\gamma|$  gives

$$\begin{aligned}
M^2 &= (E_\mu + E_\gamma)^2 - (\mathbf{p}_\mu + \mathbf{p}_\gamma) \cdot (\mathbf{p}_\mu + \mathbf{p}_\gamma) \\
&= E_\mu^2 - p_\mu^2 + E_\gamma^2 - p_\gamma^2 + 2E_\mu E_\gamma - 2p_\mu p_\gamma \cos \theta_{\mu\gamma} \\
&= m_\mu^2 + 2p_\gamma(E_\mu - p_\mu \cos \theta_{\mu\gamma}) \\
&= m_\mu^2 + 2p_\gamma p_\mu \left( \sqrt{1 + \left(\frac{m_\mu}{p_\mu}\right)^2} - \cos \theta_{\mu\gamma} \right), \tag{4}
\end{aligned}$$

where  $\theta_{\mu\gamma}$  is the angle between  $\mathbf{p}_\mu$  and  $\mathbf{p}_\gamma$ , and I have used  $E^2 = p^2 + m^2$ . This last formula involves the muon mass and the 3-momenta of the two particles, all of which we know or measure. A Monte Carlo simulation described below shows that a judicious choice of invariant mass range in  $\text{GeV}/c^2$  is  $1.73 < M < 1.82$  (see fig. 2)<sup>1</sup>.

I can derive another kinematic cut from conservation of each component of 4-momentum. Following BELLE protocol, I define the positive z-axis to point in the direction of the electron's momentum. Since the electron is more energetic than the positron, the CM frame is moving along the positive z-axis relative to the lab frame. The two  $\tau$ 's must emerge back-to-back to conserve 4-momentum in the CM frame, but the CM motion in the lab frame will add a forward z-component to each observed laboratory 3-momenta. It is possible to analyze this situation in the CM frame and then Lorentz boost to the lab frame, but I choose to work in the lab frame for concreteness. I choose the y-axis so that the  $e^+e^-$  and  $\tau^+\tau^-$  trajectories all lie in the yz-plane. Let  $\theta_{z_1}$  and  $\theta_{z_2}$  be the angles between the 3-momentum of each  $\tau$  and the z-axis. The total momentum before the collision is:

$$\vec{p}_b = \vec{p}_{e^-} + \vec{p}_{e^+} = (E_- + E_+, E_- - E_+, 0, 0), \tag{5}$$

---

<sup>1</sup>All signal plots represent a simulation with  $5 \times 10^4$  events, and with only those events displayed that survived the prior cuts as listed in table 2. Background plots show the result of a simulation with  $5 \times 10^5$  events and no cuts.

where  $E_+$  and  $E_-$  denote the electron and positron energy respectively. Note that  $E$  determines  $p$  through  $E^2 = p^2 + m^2$ , and with beam energies of  $\sim$  GeV, the electron mass of  $0.511 \text{ MeV}/c^2$  is negligible. From the geometry,

$$\vec{p}_a = \vec{p}_{\tau^+} + \vec{p}_{\tau^-} = (E_1 + E_2, 0, p_1 \sin \theta_{z_1} + p_4 \sin \theta_{z_2}, p_1 \cos \theta_{z_1} + p_2 \cos \theta_{z_2}). \quad (6)$$

Conservation of 4-momentum gives  $\vec{p}_b = \vec{p}_a$ . Working out the algebra, I solve for the magnitude of the  $\tau$  3-momentum:

$$p_i = \frac{AB + \Sigma \sqrt{B^2 + (mC)^2}}{C^2} \simeq \frac{B}{\Sigma - A} + 0.335, \quad \text{where} \quad (7)$$

$$\Sigma = E_- + E_+, \quad A = (E_- - E_+) \cos \theta_{z_i}, \quad B = 2E_- E_+, \quad \text{and} \quad C = \Sigma^2 - A^2.$$

In the limit where  $m_\tau = 0$ , this reduces to  $p_{i0} = B/(\Sigma - A)$ . Using BELLE's beam energies gives  $|p_i - p_{i0} - 0.335| < 0.001 \text{ GeV}/c$  for all  $\theta_{z_i}$ , so I use the approximation  $p_i \simeq p_{i0} + 0.335$  for simplicity. This relation between the magnitude of the reconstructed  $\tau$  momentum and its angle with the z-axis serves as the second kinematic cut. Studying the Monte Carlo output in fig. 3, I decide to require the  $\tau$  momentum to be within  $0.1 \text{ GeV}/c^2$  of the value predicted from  $\theta_z$ .

The third cut is not a strict equality, but comes from the exact differential cross-section of the electromagnetic  $e^+e^-$  interaction. In the CM frame of the decaying  $\tau$ , the  $\mu$  and  $\gamma$  are emitted back-to-back. However, the  $\tau$  is moving relative to the lab frame, with momentum typically of order  $\text{GeV}/c$ . When we transform the scattering angle of  $180^\circ$  in the CM frame back to the lab frame, the  $\tau$  momentum gets added to that of the  $\mu$  and  $\gamma$ , resulting in a small lab opening angle  $\theta_{\mu\gamma}$ . A detailed calculation of the relative frequency of a given opening angle requires a quantum electrodynamics calculation and is beyond our purposes. Fig. 4 displays  $\theta_{\mu\gamma}$  for all signal events which survive the first two cuts, and background events with no pre-cuts. Given the substantial reduction in noise events to be gained by

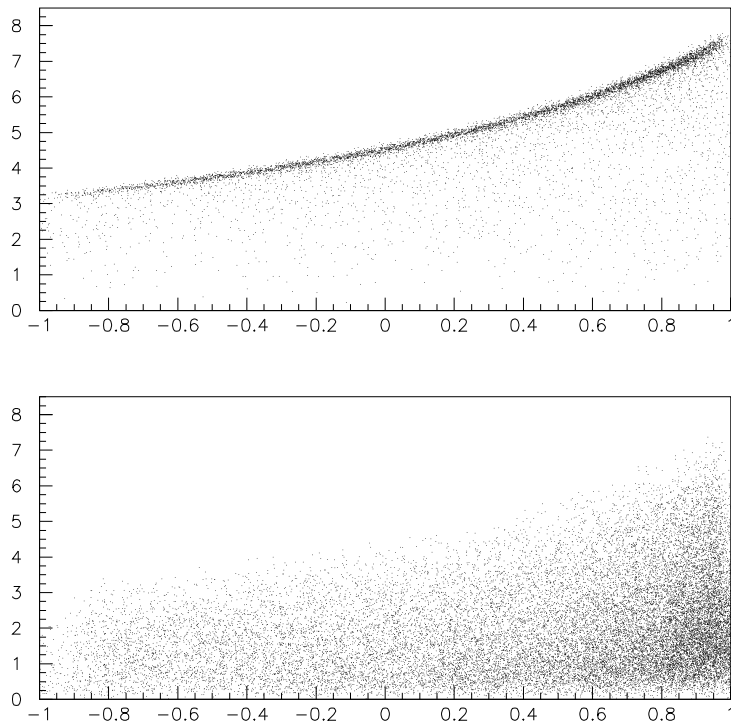


Figure 3: Reconstructed  $\tau$  momentum ( $\text{GeV}/c$ ) vs.  $\cos\theta_z$ , signal above background.

rejecting large opening angles, I choose to require  $0.1 < \cos\theta_{\mu\gamma} < 0.9$  and accept a tiny loss of signal events. Note the kinematic edge prevents opening angles very near  $0^\circ$ : only a  $\tau$  velocity of  $c$  could completely close a  $180^\circ$  CM angle to  $0^\circ$  in the lab frame.

My final cuts pertain to the photon energy and muon momentum. Besides  $\pi^0$ 's, the major source of photons in the background events that survive the above cuts originate from bremsstrahlung emitted by the initial  $e^+$  or  $e^-$ . In Monte Carlo signal events, the  $\gamma$  energy distribution was significant from 0.5 to 7.0 GeV. To reduce the bremsstrahlung events, I cut all  $\mu\gamma$  pairs where the photon energy does not fall in this range. This should be of particular help in eliminating background events with low photon energy, since the spectrum of bremsstrahlung goes like  $1/E_\gamma$ . Examining the muon momentum spectra also reveals a rapid falling-off of background events with increasing momentum, and leads me to reject events with  $p_\mu < 0.6 \text{ GeV}/c$ .

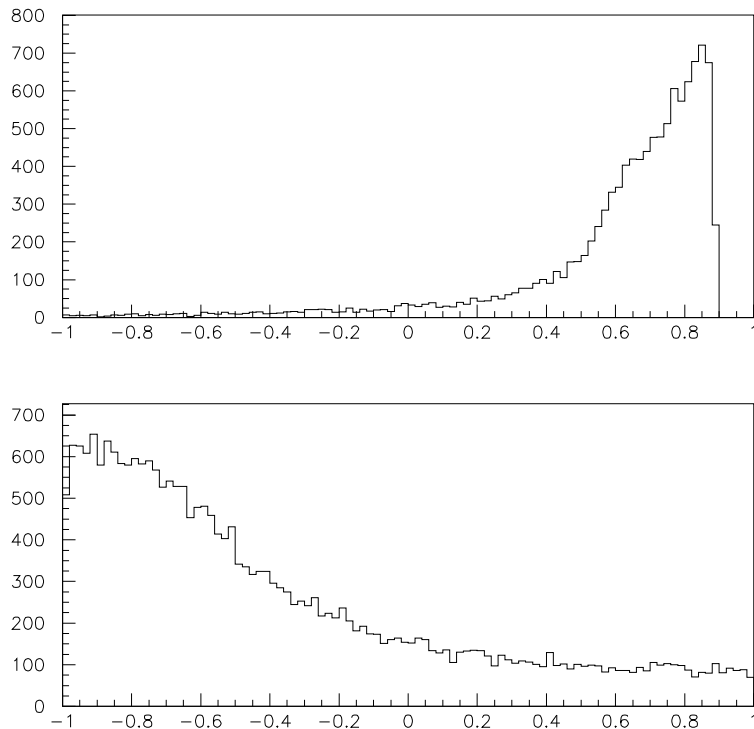


Figure 4:  $\cos\theta_{\mu\gamma}$  spectrum, signal above background.

To determine good numerical ranges for the cuts, and the resulting signal acceptance and background level, I perform a Monte Carlo simulation of the BELLE detector. Given the physical design of the detector, one could calculate the probability that, say, a given  $\tau$  will decay in a certain way and that BELLE will measure the momenta of the end products to be within some range. Although possible, this is certainly not easy. The Monte Carlo technique is the method of choice for doing this type of analysis. Whenever there can be more than one physical outcome to some process in the experiment, one assigns a range within some numerical interval (say 0 to 1) to each outcome based on the theoretical probability that it occurs. For instance, to decay a  $\tau$ , one divides an interval into ranges proportional to the branching ratio for each possible decay, and then generates a random number in the interval to determine which decay actually happens. The simulation also takes into account the physical workings of measurement devices, smearing the final results as they would be

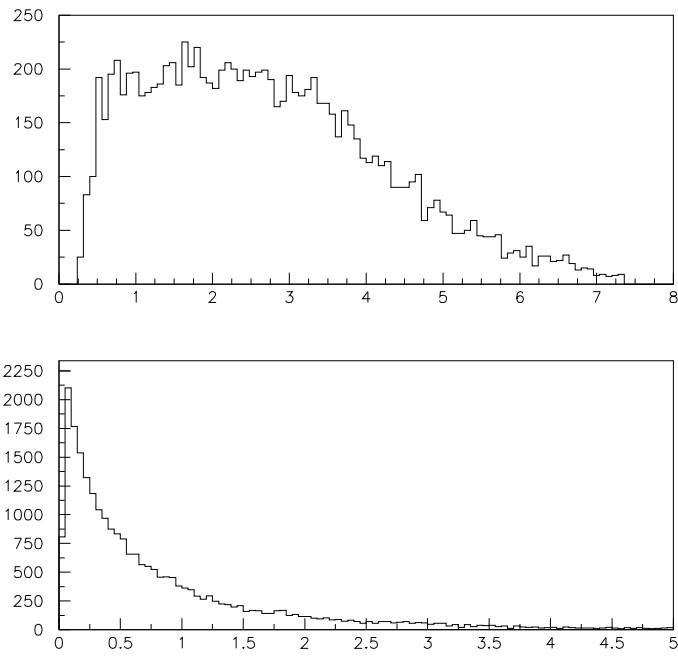


Figure 5: Photon energy spectrum (GeV), signal above background.

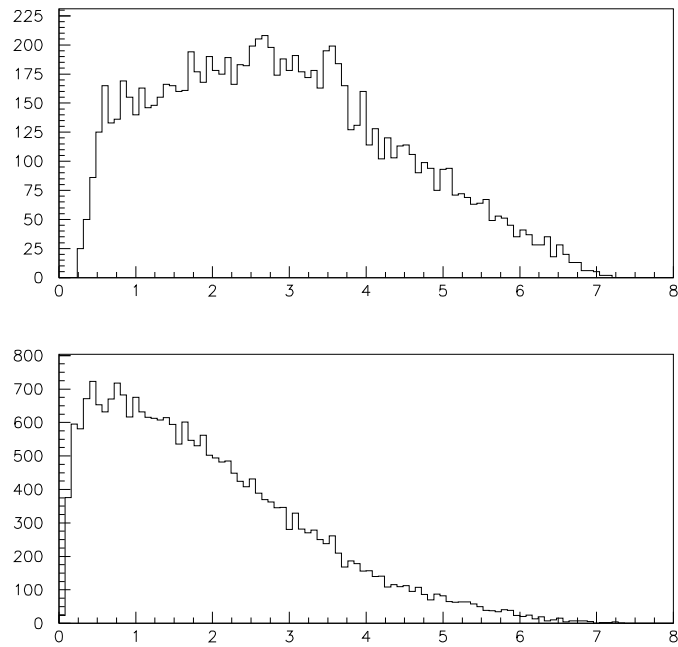


Figure 6: Muon momentum spectrum (GeV/c), signal above background.

Table 2: Effect of Cuts on Monte Carlo Events.

Cut No.	Description	Signal	Background
0	no cuts	25,119	24,779
1	$\tau$ invariant mass	16,558	603
2	$\tau$ momentum	11,096	15
3	$\mu\gamma$ opening angle	10,297	4,090
4	$\gamma$ energy	10,008	12,339
5	$\mu$ momentum	9,638	20,838

in the real experiment. Monte Carlo techniques must make simplifying assumptions, usually by treating the particles as classical projectiles and modeling the errors of some devices by gaussian smearing.

The first Monte Carlo simulation I performed is a run of only signal events, where I force the  $\tau^+$  to always decay to  $\mu^+\gamma$  via a generic phase-space decay using the relativistic Fermi's Golden Rule [7]. I produce  $\tau$  pairs using the KORALB package [8] within the BELLE Analysis Software Framework (BASF) [9], and simulate the experiment with the qq [10] and fast simulator (fsim) [11] modules and my own analysis module. The initial data acquisition routine only accepts events where the detected particles match one of the 7 final states in table 1, and only considers those photons which do not reconstruct to the  $\pi^0$  mass when paired with any other photon. I used a simulation with  $5 \times 10^4$   $\tau$  pairs to select cut ranges, and then performed a separate run with different random number seeds to determine the combined effect of the cuts. Table 2 and figs 2-6 show the effect of the cuts on this second run. I define the acceptance  $\alpha$  of my algorithm to be (num. signal events detected)/(num. signal events produced), and find that  $\alpha = 19.3\%$ .

## 4 Statistical Analysis

Having developed a set of cuts with an acceptance (19.3%) comparable to CLEO's 20.5%, I now must determine how this analysis routine acts on the results of an actual BELLE run. As mentioned above, this Monte Carlo simulation is based entirely on the current SM, which forbids  $\tau \rightarrow \mu\gamma$ . The number of  $\mu\gamma$  pairs that survive our analysis therefore represents a background level that will be present even if the decay we are looking for does not occur in nature. Of the  $5 \times 10^5$  background events generated when selecting values for the cuts and displayed in figs.2-6, none survived every cut. I then performed a simulation with  $10^8$   $\tau$  events, the expected total yield of the scheduled BELLE experiment. After applying all the cuts,  $N_b = 9$  events survived. This then is the nominal background number of events.

How does this translate into an upper limit on the branching ratio  $r$  for  $\tau \rightarrow \mu\gamma$ ? Recall that the branching ratio for a given decay is simply the probability that when a  $\tau$  decays, it will decay by this process. If we were to produce  $N$   $\tau$  pairs many times, the average number of  $\mu\gamma$  decays that would occur is then  $2Nr$ . Since the number of decays is in reality always an integer, the outcome of repeated experiment will follow the Poisson distribution [12]. The Poisson distribution gives the probability  $f$  of finding  $n$  events in some range of  $x$  (say space) given that the events occur independently of each other and of  $x$  with the average rate  $r$  as:

$$f[n, r] = \frac{r^n e^{-r}}{n!}. \quad (8)$$

It is hard to imagine a mechanism by which the decay of one  $\tau$  could be coupled either to its location or motion in space, or to the recent decays of other  $\tau$ 's in the same vicinity. Therefore, the conditions obtain for us to treat the  $\tau$  decay as a Poisson process.

Rather than consider the statistics behind directly measuring the  $\mu\gamma$  branching ratio  $r$ , it is more useful to look at what upper limit we can place on  $r$  given an average number of background events  $N_b$ . Let us first consider the case of no background and complete acceptance. Defining  $N_o$  and  $N_s$  to be the number of total observed and observed signal

events, we have  $N_o = N_s = 2Nr$ . The general idea is to assume the “worst-case scenario:” our experiment happened to produce an inordinately small number of signal events for the true  $r$ . In this situation,  $r$  would be large enough that the probability of detecting  $N_s$  or less signal events is small. We choose a confidence level (C.L.)  $1 - \epsilon$  and find the  $r$  that leads to a  $1 - \epsilon$  probability that a given experiment would detect more than the  $N_s$  events we measured. Mathematically, we want to find  $r$  so that

$$1 - \epsilon = \sum_{n=N_s+1}^{\infty} f[n, r]. \quad (9)$$

We must now take into account the effects of the background level  $N_b$  and of the finite signal acceptance  $\alpha$ . In this case,

$$N_s = 2Nr\alpha, \quad \text{and} \quad N_o = N_s + N_b = 2Nr\alpha + N_b. \quad (10)$$

Given  $N_s$ , the “true” branching ratio is then

$$r = \frac{N_s}{\alpha N}. \quad (11)$$

Extracting  $N_s$  from  $N_o$  in the presence of background is treacherous, but the general idea is still to assume we produced an unusually low number of signal events, and then find a value of  $r$  that yields this number  $\epsilon$  of the time. It suffices for our purposes to quote the result of this analysis given in [12]:

$$\epsilon = \frac{e^{-(N_s+N_b)} \sum_{n=0}^{N_o} \frac{(N_s+N_b)^n}{n!}}{e^{-N_b} \sum_{n=0}^{N_o} \frac{N_b^n}{n!}}. \quad (12)$$

To get an idea of what kind of upper limit my analysis routine lets us set on  $r$ , suppose we observe one standard deviation more events than background. For any counting experiment which follows the Poisson distribution, we know that the error on a measured value  $m$  is just  $\sigma_m = \sqrt{m}$ . This yields  $N_o = N_b + \sigma_b = 12$ . We can then deduce at  $1 - \epsilon = 90\%$  C.L. that

$N_s$  is at most 9.1, which gives  $r \leq 4.7 \times 10^{-7}$ . This would be a factor of  $\sim 9$  improvement over the CLEO upper limit of  $4.2 \times 10^{-6}$ .

Although the precise statistical treatment here is rather subtle, a few limiting cases are clear. If the true  $r$  is sufficiently small,  $N_o \simeq N_b$ , and it will be impossible to extract its exact *value* from the background. On the other hand, if  $r$  dwarfs the background, it will be easy to detect. The two extremes converge and make for a complex situation near the “background” branching ratio  $N_b/N$ , which for 9 background events is  $9 \times 10^{-8}$ . An effective way to see what kind of  $r$  we can detect is to consider a quantity called the significance  $S$  as a function of  $r$ . I define

$$S \equiv \frac{N_s}{\sigma_s}, \quad (13)$$

where  $\sigma_s$  is the error on  $N_s$ . Propagation of error dictates that

$$\sigma_s^2 = \left(\frac{\partial N_s}{\partial N_o}\right)^2 \sigma_o^2 + \left(\frac{\partial N_s}{\partial N_b}\right)^2 \sigma_b^2 = \sqrt{N_o + N_b}, \quad (14)$$

where  $\sigma_o$  and  $\sigma_b$  are the errors on  $N_o$  and  $N_b$  respectively. For the significance, this gives

$$S = \frac{N_s}{\sigma_s} = \frac{(N_o - N_b)}{\sqrt{N_o + N_b}} = \frac{2Nr\alpha}{\sqrt{2Nr\alpha + 2N_b}}, \quad (15)$$

where I have substituted  $N_o = 2Nr\alpha + N_b$ . Fig. 7 shows significance versus branching ratio for  $10^8$  events and a background of 9. A 90% C.L. corresponds to a significance of 1.64, which shows that my algorithm can detect a branching ratio of  $2.2 \times 10^{-7}$  at that C.L. Note that for an  $r$  slightly lower than the CLEO upper limit, say  $r = 4 \times 10^{-6}$ , the significance is quite high:  $S = 12.1$ .

## 5 Conclusion and Future Prospects

The results of Monte Carlo simulations presented in this paper strongly suggest that the BELLE experiment offers the opportunity to increase the upper limit on the  $\tau \rightarrow \mu\gamma$  branch-

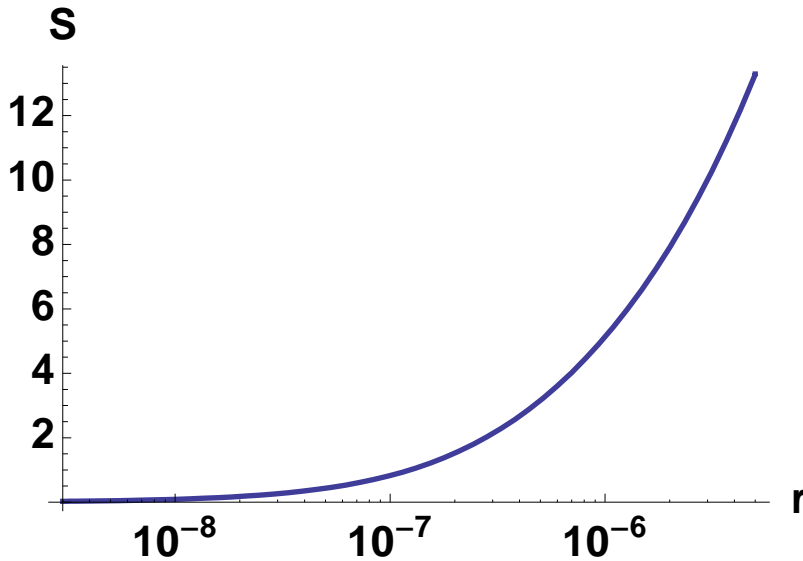


Figure 7: Significance (S) vs. Branching Ratio (r),  $N = 10^8$ ,  $N_b = 9$

ing ratio by at least an order of magnitude. They show that the analysis procedure I use identifies 9 background events in a sample of  $10^8$   $\tau$  pairs and accepts 19.3% of signal events. Nonetheless, there is room for improvement in the analysis algorithm. Most importantly, the cuts pass a nonzero number of background events, which greatly complicates the statistics and lowers the potential upper limit improvement. Unfortunately, it seems hard to imagine new kinematic cuts that would do this without severely degrading the signal acceptance. Since my acceptance is slightly worse than that of CLEO and my background level is consistent with theirs when scaled, it is possible that I am just inside a regime where there is simply an irreducible background level, and the CLEO group was just outside it. Another concern is that I have dismissed events where the initial virtual photon decays by another channel, such as into a quark-antiquark pair, as not contributing anything to the background level. This is not clear *a priori*, and should be explored in further simulations.

Regardless of theoretical bias, the search for lepton flavor violation may provide a doorway to new physics, and certainly to a phenomenon not explained by the Standard Model. Besides simply accounting for this process, any acceptable theory must also explain why, if allowed, it is so incredibly rare. As with all domains not yet explored experimentally, there is the possibility that Nature holds something unexpected in store for us. In a way, it is upsetting

that some extensions to the Standard Model already call for lepton flavor violation: the unanticipated demon, lurking just beyond the pale of the human imagination, creates the largest tremors in our intellectual edifice.

## References

- [1] S. Kelley et al. *Nuclear Physics*, 27, 1991.
- [2] R. Arnowitt and P. Nath. *Physical Review Letters*, 66:2708, 1991.
- [3] CLEO Collaboration. *Physical Review Letters*, 70:138, 1993.
- [4] G. L. Kane. *Modern Elementary Particle Physics: the Fundamental Particles and Forces?* Addison-Wesley Publishing Company, updated edition, 1987.
- [5] D. H. Perkins. *Introduction to High Energy Physics*. Addison-Wesley Publishing Company, 3rd edition, 1987.
- [6] The BELLE Collaboration. Belle technical design report. Technical report, National Laboratory for High Energy Physics, 1995.
- [7] D. J. Griffiths. *Introduction to Elementary Particles*. John Wiley & sons, Inc., 1987.
- [8] S. Jadach and Z. Was. *Computational Physics Communications*, 85:453, 1995.
- [9] R. Itoh. *BASF User's Manual*. Physics Division, KEK, December 1996.
- [10] K. Lingel. *QQ Documentation Sources*. [www.lns.cornell.edu/public/CLEO/soft/qq/](http://www.lns.cornell.edu/public/CLEO/soft/qq/).
- [11] H. Ozaki. *Belle Note #99: FSIM V5.0*. KEK, February 1996.
- [12] Particle Data Group. *Review of Particle Properties*. American Physical Society, 1994.

*This paper represents my own work, written in accordance with University regulations.*